

Chiral Symmetry Breaking and Scalar Confinement

P. Bicudo* and G. M. Marques†

Dep. Física and CFIF, Instituto Superior Técnico, Av. Rovisco Pais 1049-001 Lisboa, Portugal

We address the old difficulty in accommodating the scalar quark-antiquark confining potential together with chiral symmetry breaking. We develop a quark confining potential inspired in the QCD scalar flux tube. The coupling to quarks consists in a double vector vertex. We study the Dirac and spin structure of this potential. In the limit of massless quarks the quark vertex is vector. Nevertheless symmetry breaking generates a new scalar quark vertex. In the heavy quark limit the coupling is mostly scalar. We solve the mass gap equation and find that this potential produces spontaneous chiral symmetry breaking for light quarks. The quantitative results of this model are encouraging.

I. INTRODUCTION

Spontaneous Chiral Symmetry Breaking ($S\chi SB$) is accepted to occur in low energy hadronic physics. Another important feature of hadronic physics, suggested by the spectroscopy of hadrons, by lattice simulations and by models of confinement is scalar confinement. However $S\chi SB$ and scalar confinement are apparently conflicting, since the first requires a chiral invariant coupling to the quarks, like the vector coupling of QCD. We address a recent quest of Bjorken [1], “how are the many disparate methods of describing hadrons which are now in use related to each other and to first principles of QCD?”. Although the vector confinement of quarks is not yet ruled out [2, 3, 4, 5], here we try to solve this old chiral symmetry versus scalar confinement conflict of hadronic physics, which remained open for many years.

In this paper we explore scalar confinement from the perspective of chiral symmetry breaking. In Section II we motivate the importance of both $S\chi SB$ and scalar confinement. We show these features of hadronic physics to have some subtle weaknesses that we capitalize to construct a model. The potential used in our Quark Model (QM) is defined in Section III. The self consistent mass gap equation for the quarks is derived in Section IV. In Section V we solve numerically the mass gap equation and calculate the quark condensate. Finally, in Section VI we present some conclusions.

II. MATCHING CHIRAL SYMMETRY BREAKING WITH SCALAR CONFINEMENT

The QCD lagrangian is chiral invariant in the limit of vanishing quark masses. Nambu and Jona-Lasinio showed that including chiral symmetry in fermionic systems provides a natural explanation for the small pion mass, which is much lighter than all the other isovector hadrons. Because of this crucial fact the mechanism of

$S\chi SB$ is accepted to occur in low energy hadronic physics for the light flavors u , d and s , where $m_u, m_d \ll m_s < \Lambda_{QCD} < M_N/3$. Similarly to the vector Ward identities in gauge symmetry, the axial Ward identities constitute a powerful tool of chiral symmetry. The techniques of current algebra led to beautifully correct theorems, the Partially Conserved Axial Current (PCAC) theorems. The different variants of QMs are widely used as simplifications of QCD. They are convenient to study quark bound states and hadron scattering. Recently [6] we have shown these beautiful PCAC theorems, like the Weinberg theorem for $\pi - \pi$ scattering, to be reproduced by QMs with $S\chi SB$. Another important benefit of having $S\chi SB$ in the QM is the reduced number of parameters. The mass gap equation generates a dynamical constituent quark mass, which is no longer an independent parameter, even for quarks with a vanishing current mass. The quark-quark, quark-antiquark, antiquark-antiquark potentials, and the quark-antiquark annihilation and creation interactions are all originated in the same chiral invariant Bethe-Salpeter kernel. Therefore any QM for light quarks should comply with the $S\chi SB$. Moreover the microscopic coupling of the quark to the confining interaction should include the vector coupling which is present in the quark-gluon vertex of QCD. However there is some evidence that a vector quark-quark potential is not sufficient to provide the expected scale of $S\chi SB$ of the order of 200 – 300 MeV which is present both in the constituent quark mass and in the quark condensate. It was realized by Adler [7] that a linear confinement with vector couplings was not sufficient to provide the correct quark condensate. Moreover the gluon propagator extracted from the lattice, when used in a one gluon exchange truncation of the quark mass gap equation, is not able to provide the expected quark condensate [8]. This also happens with the gluon propagator extracted from the solution of truncated Schwinger-Dyson equations of QCD [9]. Importantly, these gluon propagators exhibit a non-perturbative mass. This mass should produce a Meissner effect in Yang-Mills fields, and this is expected to produce a confining string for the quarks. Here we will estimate the effect of the confining string on the quark condensate.

On the other hand the confining potential for con-

*Electronic address: bicudo@ist.utl.pt

†Electronic address: gmarques@cfif.ist.utl.pt

stituent quarks is probably scalar. We can learn much by comparing simply the spectrum of the hydrogen atom with the masses of all hadron families. In a perturbative QCD scenario, the hadron spectroscopy would be dominated by the one gluon exchange, which is qualitatively similar to the one photon exchange interaction that explains in detail atomic physics. It turns out that all the hadronic families, say of mesons or baryons, with light or heavy flavors, show similar differences with the hydrogen spectrum. It is remarkable that the Spin-Orbit potential (also called fine interaction in atomic physics) turns out to be suppressed in hadronic spectra since it is smaller than the Spin-Spin potential (hyperfine interaction). This constitutes an evidence of non-perturbative QCD. Another evidence of non-perturbative QCD is present in the angular and radial excitations of hadrons, which fit linear trajectories in Regge plots, and suggest a long range, probably linear, confining potential for the quarks. This led Henriques, Kellett and Moorhouse [10] to develop a QM where a short range vector potential and a long range scalar potential partly cancel the Spin-Orbit contribution. The short range potential is Coulomb-like (inspired in the one gluon exchange) and its quark vertex has a vector coupling structure $\bar{\psi}\gamma^\mu\psi$. The long range potential has scalar coupling $\bar{\psi}\psi$ and is a linear potential [10, 11, 12, 13].

The same scalar confinement picture is extracted from lattice simulations. In quenched lattices which simulate the quark-antiquark potential in the heavy quark limit, the pattern of spin-spin, tensor, and spin-orbit interactions is compatible with a scalar confinement [14, 15, 16]. Moreover the presently favored confinement picture in the literature is the flux tube, or string picture, with tension $\sigma \simeq 200$ MeV/Fm. Quantum mechanics suggests that a thin string, in its ground-state, should be a scalar object [17]. Only higher energy excitations of the string would have angular momentum. This was capitalized by Isgur and Paton in the flux tube model [18].

In this paper we will assume the quarks are coupled to a scalar object which provides a linear confinement. On top of that we want this coupling to use, as a microscopic building block, the vector gluon-quark which is present in QCD. Notice that to get a Lorentz scalar coupling a simple one gluon vertex is not enough. The coupling needs at least two vertices. The simplest way to achieve this is to have the string emitting two effective gluons that couple to the same quark line. This double vertex, coupling the string to a quark line via two intermediate gluon propagators, is presented in Fig. 1. Effectively this double vertex is similar to the vertices that couple a quark to a gluon ladder in the soft pomeron models [19, 20]. It is also related to the light quark vertex in the heavy-light quark bound states studied in the local gauge coordinate [21, 22, 23]. Such a double vertex was also introduced in the coupling of short strings to quarks [24]. In the cumulant expansion formalism in terms of gluon correlators [21, 25] this means the quark-antiquark coupling will be dominated by four gluon correlators.

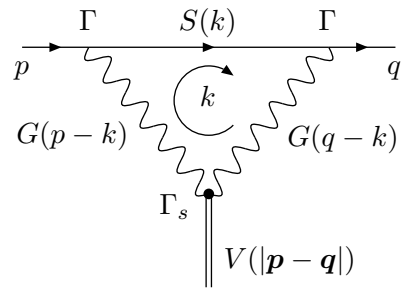


FIG. 1: The coupling of a quark to a string with a double gluon vertex

III. THE DOUBLE VERTEX NON-PERTURBATIVE CONFINING INTERACTION

In this section we construct the simplest possible coupling, that simulates that of a quark line with a scalar string using two vector couplings as building blocks. The most general coupling of this kind is presented in Fig. 1 and it is simply read,

$$\int \frac{d^4k}{(2\pi)^4} (\Gamma V^a) S(k) (\Gamma V^b) G^{bc}(p-k) (\Gamma_S W^{cde}) G^{ad}(q-k), \quad (1)$$

where Γ is the Dirac structure of the fermion-gluon interaction and V^a the usual color interaction $\lambda^a/2$. We denote the quark propagator by $S(k)$ and the gluon propagator by $G^{ab}(k)$. Finally $\Gamma_S W^{cde}$ represents the coupling of the gluon pair to the string.

To get the coupling of the string to a light quark, we follow the coupling obtained in the heavy-light quark system, computed in the local coordinate gauge [22]. This model interpolates between the heavy-light meson in the local gauge and the effective QM. So, for the Dirac structure of the quark-gluon sub-vertices Γ we have γ^0 matrices, which is also compatible with the Coulomb gauge.

In the color sector, as already stated, the coupling of the same sub-vertices has a $\lambda^a/2$ structure, where λ^a are the Gell-Mann matrices. The remaining sub-vertex includes the coupling of two color octets, see Fig. 2. The string is also a colored object; it contains a flux of color-electric field. For a scalar coupling, which is symmetric, we use the symmetric structure function d^{abc} defined by

$$\{\lambda^a, \lambda^b\} = \frac{4}{3} \delta^{ab} + 2 d^{abc} \lambda^c. \quad (2)$$

This will result in a color contribution for the effective vertex of

$$d^{abc} \frac{\lambda^b}{2} \cdot \frac{\lambda^c}{2} = \mathcal{C} \frac{\lambda^a}{2}, \quad \mathcal{C} = \frac{5}{6}. \quad (3)$$

In QMs the string usually couples to the quark line with a $\lambda^a/2$. In our case it couples with two $\lambda^a/2$, one for

$$\begin{array}{|c|c|} \hline \square & \square \\ \hline \square & \square \\ \hline \end{array} \times \begin{array}{|c|c|} \hline \square & \square \\ \hline \square & \square \\ \hline \end{array} = \begin{array}{|c|c|c|c|} \hline \square & \square & \square & \square \\ \hline \square & \square & \square & \square \\ \hline \end{array} + \begin{array}{|c|c|c|c|} \hline \square & \square & \square & \square \\ \hline \square & \square & \square & \square \\ \hline \end{array} + \begin{array}{|c|c|} \hline \square & \square \\ \hline \square & \square \\ \hline \end{array} + \begin{array}{|c|c|} \hline \square & \square \\ \hline \square & \square \\ \hline \end{array} + \begin{array}{|c|c|} \hline \square & \square \\ \hline \square & \square \\ \hline \end{array} + \begin{array}{|c|c|} \hline \square & \square \\ \hline \square & \square \\ \hline \end{array} + \textcircled{1}$$

$$8 + 8 = 27 + 10 + \overline{10} + 8 + 8 + 1$$

FIG. 2: String color

each sub-vertex. But as we can see from (3) the effective result is the same.

The gluon propagators and the different sub-vertices result in a distribution in the loop momentum k . Here different choices would be possible. For simplicity we assume that the relative momentum $p - q$ flows equally in the two effective gluon lines. We also remark that the distribution in k is normalized to unity once the correct string tension is included in the relative potential $V(p - q)$. This amounts to consider that the momentum k distribution is a Dirac delta

$$(2\pi)^3 \delta^3 \left(\mathbf{k} - \frac{\mathbf{p} + \mathbf{q}}{2} \right). \quad (4)$$

If we summarize the above assumptions in a formula the loop vertex that will be used is

$$\int \frac{d^4 k}{(2\pi)^4} \left(\gamma^0 \frac{\lambda^a}{2} \right) S(k) \left(\gamma^0 \frac{\lambda^b}{2} \right) d^{abc} (2\pi)^3 \delta^3 \left(\mathbf{k} - \frac{\mathbf{p} + \mathbf{q}}{2} \right). \quad (5)$$

The equal-time approximation, which is standard in QMs, allows the computation of the double vertex as a functional of the running quark mass m_k . The quark mass will be computed self-consistently in the next sections.

We decompose the fermion propagator in the usual particle and antiparticle propagators

$$\begin{aligned} S(k) &= \frac{i}{k - m_k + i\epsilon} \\ &= \frac{i\Lambda^+(\mathbf{k})\beta}{k_0 - E_k + i\epsilon} - \frac{i\Lambda^-(\mathbf{k})\beta}{-k_0 - E_k + i\epsilon} \end{aligned} \quad (6)$$

where the quark energy projectors are

$$\begin{aligned} \Lambda^+(\mathbf{k}) &= \frac{1 + s_k \beta + c_k \hat{\mathbf{k}} \cdot \boldsymbol{\alpha}}{2} = \sum_s u_s(k) u_s^\dagger(k) \\ \Lambda^-(\mathbf{k}) &= \frac{1 - s_k \beta - c_k \hat{\mathbf{k}} \cdot \boldsymbol{\alpha}}{2} = \sum_s v_s(k) v_s^\dagger(k) \end{aligned} \quad (7)$$

and where $s_k = \sin \varphi_k = m_k / \sqrt{k^2 + m_k^2}$, $c_k = \cos \varphi_k = k / \sqrt{k^2 + m_k^2}$ and φ_k is the chiral angle, a convenient function for algebraic and numerical computations.

The energy loop integral can be easily calculated,

$$\int \frac{dk^0}{2\pi} \frac{i}{k^0 \mp E \pm i\epsilon} \Lambda^\pm \beta = \pm \Lambda^\pm \beta \quad (8)$$

$$\begin{aligned} \int \frac{dk^0}{2\pi} S(k) &= (\Lambda^+ - \Lambda^-) \beta \\ &= (s_k \beta + c_k \hat{\mathbf{k}} \cdot \boldsymbol{\alpha}) \beta \end{aligned} \quad (9)$$

Finally, using the Dirac delta distribution for the remaining integrals over the three momentum \mathbf{k} , and summing in color indices, we get the following effective vertex,

$$\mathcal{V}_{\text{eff}} = \mathcal{C} \frac{\lambda^c}{2} (s_k - c_k \hat{\mathbf{k}} \cdot \boldsymbol{\gamma}) \Big|_{k=\frac{p+q}{2}}. \quad (10)$$

In the remainder of the paper we will always assume $k = (p + q)/2$.

Eq. (10) shows that the double vertex actually solves the problem of matching chiral symmetry breaking and scalar confinement. In the chiral limit of a vanishing quark mass, the effective vertex $\mathcal{V}_{\text{eff}} \rightarrow -\mathcal{C} \lambda^c / 2 \hat{\mathbf{k}} \cdot \boldsymbol{\gamma}$ is proportional to the γ^μ and is therefore chiral invariant as it should be, whereas in the heavy quark limit, $\mathcal{V}_{\text{eff}} \rightarrow \mathcal{C} \lambda^c / 2$ is simply a scalar vertex. The Gell-Mann matrix λ^c provides the usual color vector coupling as expected in a QM. We anticipate that the dynamical generation of a quark mass will also generate a scalar coupling for light quarks, and this results in an effective vertex, including a chiral invariant vertex \not{p} and the standard scalar vertex 1.

The dependence in the relative momentum must comply with the linear confinement which is derived from the string picture,

$$\mathbf{V}_\varepsilon(\mathbf{x}) = \frac{16}{3\mathcal{C}^2} V_\varepsilon(\mathbf{x}) = \frac{16}{3\mathcal{C}^2} \sigma |\mathbf{x}| e^{-\varepsilon |\mathbf{x}|}, \quad (11)$$

where $\sigma \simeq 200$ MeV/Fm is the string constant and \mathcal{C} is the algebraic color factor defined in Eq. (3). The damping factor ε regularizes the Fourier transform,

$$\mathbf{V}_\varepsilon(\mathbf{p}) = -\frac{16}{3\mathcal{C}^2} 8\pi\sigma \left(\frac{1}{(|\mathbf{p}|^2 + \varepsilon^2)^2} - \frac{4\varepsilon^2}{(|\mathbf{p}|^2 + \varepsilon^2)^3} \right), \quad (12)$$

and in the limit $\varepsilon \rightarrow 0$ we have

$$-i V_0(\mathbf{p} - \mathbf{q}) = -i \frac{-8\pi\sigma}{|\mathbf{p} - \mathbf{q}|^4}. \quad (13)$$

IV. MASS GAP EQUATION

We solve the mass gap equation using the Schwinger-Dyson formalism,

$$S^{-1} = S_0^{-1} - \Sigma, \quad (14)$$

where the dressed propagator is defined in eq. (6) and the free propagator has a similar definition with the quark bare mass m_0 . We want to determine the constituent

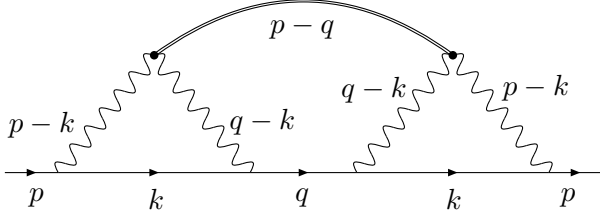


FIG. 3: The self-energy term of the mass gap equation

quark mass m_p solving the self consistent mass gap equation. To compute the self energy in this model, using the effective string potential which couples to the quark line with double vertices, we have to deal with the three loop diagram of Fig. 3. Keeping in mind that the two double vertex loops are already simplified. Technically other diagrams, with crossed gluon legs, could exist but we assume that this is the dominant diagram.

The mass gap equation can be much simplified in the spin formalism. Some useful relations we will use for this purpose are

$$\begin{aligned}
u_s^\dagger(p) v_{s'}(p) &= \mathbf{0} \cdot [\boldsymbol{\sigma}(i\sigma_2)]_{ss'} \\
u_s^\dagger(p) \beta v_{s'}(p) &= c_p \hat{\mathbf{p}} \cdot [\boldsymbol{\sigma}(i\sigma_2)]_{ss'} \\
u_s^\dagger(p) \alpha^i v_{s'}(p) &= -(\delta^{ij} - (1-s_p) \hat{p}^i \hat{p}^j) [\sigma^j(i\sigma_2)]_{ss'} \\
u_s^\dagger(p) \beta \alpha^i v_{s'}(p) &= -(s_p \delta^{ij} + (1-s_p) \hat{p}^i \hat{p}^j) [\sigma^j(i\sigma_2)]_{ss'}
\end{aligned} \tag{15}$$

With eqs. (6), (7) and (15) we arrive at the expected relation [26]

$$\bar{u}_s(p) S^{-1}(p) v_{s'}(p) = 0, \tag{16}$$

implying that the propagator is diagonal in the particle-antiparticle projection. The mass gap equation becomes

$$\bar{u}_s(p) S_0^{-1}(p) v_{s'}(p) - \bar{u}_s(p) \Sigma(p) v_{s'}(p) = 0. \tag{17}$$

The free propagator term for a zero bare mass, $m_0 = 0$, is simply

$$u_s^\dagger(p) \beta (-i) \not{p} v_{s'}(p) = ip s_p \hat{\mathbf{p}} \cdot [\boldsymbol{\sigma}(i\sigma_2)]_{ss'} \tag{18}$$

The self-energy term is directly derived from the diagram of Fig. 3 using the double vertex loop \mathcal{V}_{eff} already obtained in (10),

$$\begin{aligned}
\Sigma(p) &= \int \frac{d^3 q}{(2\pi)^3} (s_k - c_k \hat{\mathbf{k}} \cdot \boldsymbol{\gamma}) (s_q \beta + c_q \hat{\mathbf{q}} \cdot \boldsymbol{\alpha}) \beta \times \\
&\quad \times (s_k - c_k \hat{\mathbf{k}} \cdot \boldsymbol{\gamma}) \mathcal{C}^2 \frac{3}{16} (-i) \mathbf{V}_\varepsilon(|\mathbf{p} - \mathbf{q}|) \\
&= \int \frac{d^3 q}{(2\pi)^3} \left((s_k^2 - c_k^2) s_q \beta - 2s_k c_k s_q \hat{\mathbf{k}} \cdot \boldsymbol{\alpha} + \right. \\
&\quad \left. + (s_k^2 + c_k^2) c_q \hat{\mathbf{q}} \cdot \boldsymbol{\alpha} + 2s_k c_k c_q \hat{\mathbf{k}} \cdot \hat{\mathbf{q}} \beta - \right. \\
&\quad \left. - 2c_k^2 c_q \hat{\mathbf{k}} \cdot \hat{\mathbf{q}} \hat{\mathbf{k}} \cdot \boldsymbol{\alpha} \right) \beta (-i) V_\varepsilon(|\mathbf{p} - \mathbf{q}|),
\end{aligned} \tag{19}$$

where we used the properties of the β and α^i matrices. The result for the mass gap self-energy term is

$$\begin{aligned}
\bar{u}_s(p) \Sigma(p) v_{s'}(p) &= \\
&= \int \frac{d^3 q}{(2\pi)^3} (-i) V_\varepsilon(|\mathbf{p} - \mathbf{q}|) \left[(s_k^2 - c_k^2) s_q (-c_p \hat{\mathbf{p}}) - \right. \\
&\quad - 2s_k c_k s_q (-\hat{\mathbf{k}} + (1-s_p) \hat{\mathbf{k}} \cdot \hat{\mathbf{p}} \hat{\mathbf{p}}) + \\
&\quad + c_q (-\hat{\mathbf{q}} + (1-s_p) \hat{\mathbf{q}} \cdot \hat{\mathbf{p}} \hat{\mathbf{p}}) + \\
&\quad + 2s_k c_k c_q \hat{\mathbf{k}} \cdot \hat{\mathbf{q}} (-c_p \hat{\mathbf{p}}) - \\
&\quad \left. - 2c_k^2 c_q \hat{\mathbf{k}} \cdot \hat{\mathbf{q}} (-\hat{\mathbf{k}} + (1-s_p) \hat{\mathbf{k}} \cdot \hat{\mathbf{p}} \hat{\mathbf{p}}) \right] \cdot [\boldsymbol{\sigma}(i\sigma_2)]
\end{aligned} \tag{20}$$

As we can see from (18) and (20) both terms of the mass gap equation are proportional to $\hat{\mathbf{p}} \cdot \boldsymbol{\sigma}(i\sigma_2)$. Since the Pauli matrices σ are linearly independent, we can substitute $\boldsymbol{\sigma}(i\sigma_2)$ by $\hat{\mathbf{p}}$ and still have a mass gap condition. With this simplification the mass gap equation reduces to,

$$\begin{aligned}
ip s_p - \int \frac{d^3 q}{(2\pi)^3} \left[(c_k^2 - s_k^2) s_q c_p + 2s_k c_k s_q s_p \hat{\mathbf{k}} \cdot \hat{\mathbf{p}} - \right. \\
\left. - c_q s_p \hat{\mathbf{q}} \cdot \hat{\mathbf{p}} - 2s_k c_k c_q c_p \hat{\mathbf{k}} \cdot \hat{\mathbf{q}} + \right. \\
\left. + 2c_k^2 c_q s_p \hat{\mathbf{k}} \cdot \hat{\mathbf{q}} \hat{\mathbf{k}} \cdot \hat{\mathbf{p}} \right] i V_\varepsilon(|\mathbf{p} - \mathbf{q}|) = 0.
\end{aligned} \tag{21}$$

Notice that if we take the integrand and set $\mathbf{q} = \mathbf{p}$ we will get $0 \times V_\varepsilon(0)$. In section V we will deal numerically with this IR behavior.

V. NUMERICAL SOLUTION OF THE MASS GAP EQUATION

The mass gap equation is a difficult non-linear integral equation, that does not converge with the usual iterative methods. We developed a method to solve the mass gap equation with a differential equation, using a convergence parameter λ . This parameter is the radius of a sphere centered in $\mathbf{u} = \mathbf{p} - \mathbf{q} = 0$ it allows us to separate the integral into an integral inside the sphere and another outside of it,

$$\begin{aligned}
\int \frac{d^3 u}{(2\pi)^3} f(\mathbf{p}, \mathbf{u}) V_\varepsilon(u) &= \int_{\circ} \frac{d^3 u}{(2\pi)^3} f(\mathbf{p}, \mathbf{u}) V_\varepsilon(u) \\
&\quad + \int_{R^3 - \circ} \frac{d^3 u}{(2\pi)^3} f(\mathbf{p}, \mathbf{u}) V_\varepsilon(u).
\end{aligned} \tag{22}$$

In our model $f(\mathbf{p}, \mathbf{u})$ is the function dependent on the chiral angle presented in eq. (21).

Let us first focus on the integral inside the sphere, where we have $u < \lambda$. Eventually we will take the limit where $\lambda \rightarrow 0$ and this term will vanish. But for now we will expand the function f around $u = 0$ and take only

the first non-vanishing term,

$$\int_{\circ} \frac{d^3 u}{(2\pi)^3} f(p, u, \omega) V_{\varepsilon}(u) \approx \int_{\circ} \frac{d^3 u}{(2\pi)^3} \frac{\partial^2 f}{\partial u^2} \Big|_{u=0} V_{\varepsilon}(u) \\ \stackrel{\varepsilon \rightarrow 0}{=} \frac{\lambda(-8\pi\sigma)}{8\pi^2} \int_{-1}^1 d\omega \frac{\partial^2 f}{\partial u^2} \Big|_{u=0}, \quad (23)$$

where ω is the cosine of the angle between \mathbf{p} and \mathbf{u} . For our particular model we have

$$\int_{-1}^1 d\omega \frac{\partial^2 f}{\partial u^2} \Big|_{u=0} = \frac{\sin(2\varphi_p) - 2p \cos(2\varphi_p) \varphi'_p + p^2 \varphi''_p}{3p^2} \quad (24)$$

In what concerns the integral outside the sphere ($u > \lambda$) we can take from the beginning $\varepsilon = 0$ since this integral is already regulated by λ . In this case we have

$$\int_{R^3 - \circ} \frac{d^3 u}{(2\pi)^3} f(\mathbf{p}, \mathbf{u}) V_0(u) = \\ = \frac{-8\pi\sigma}{4\pi^2} \int_{\lambda}^{\infty} du \int_1^{-1} d\omega \frac{1}{u^2} f(p, u, \omega). \quad (25)$$

Placing the two terms in the mass gap equation we finally get the equation that we can iterate to find the solution,

$$3p s_p + \frac{\sigma}{\pi} \left[\lambda \left(\varphi''_p - \frac{2}{p} \cos(2\varphi_p) \varphi'_p + \frac{1}{p^2} \sin(2\varphi_p) \right) + 6 \int_{\lambda}^{\infty} du \int_1^{-1} d\omega \frac{1}{u^2} f(p, u, \omega) \right] = 0 \quad (26)$$

Our technique consists in starting with a large infrared cutoff λ , where the integral term of Eq. (26) is negligible. In this case Eq. (26) for the chiral angle φ_p becomes essentially a differential equation which can be solved with the standard shooting method [27]. It turns out that this equation possesses several solutions, and we specialize in the larger one, with no nodes, that corresponds to the stable vacuum [28]. Then one decreases step by step the λ parameter, using as an initial guess for the evaluation of the integral the φ_p determined for the previous value of λ . In this way the integral is a simple function of the momentum p and we again have to solve a non-homogeneous differential equation. Eventually we are able to solve the mass gap equation for a λ parameter which is much smaller than the scale of the interaction. Finally we extrapolate the set of obtained φ_p to the limit of $\lambda \rightarrow 0$. We test the convergence of the method computing the quark condensate $\langle \bar{\psi}\psi \rangle$,

$$\langle \bar{\psi}\psi \rangle = 6 \int \frac{d^3 p}{(2\pi)^3} s_p. \quad (27)$$

The evolution of the solution as a function of the infrared parameter λ is clearer when we display the quark condensate, see Fig. 4.

The solution of the mass gap equation is presented in Fig. 5, where we compare it with the single vertex model solution.

VI. RESULTS AND CONCLUSION

In this paper we build a QM for the coupling of quark to a scalar string. The quark confining interaction has

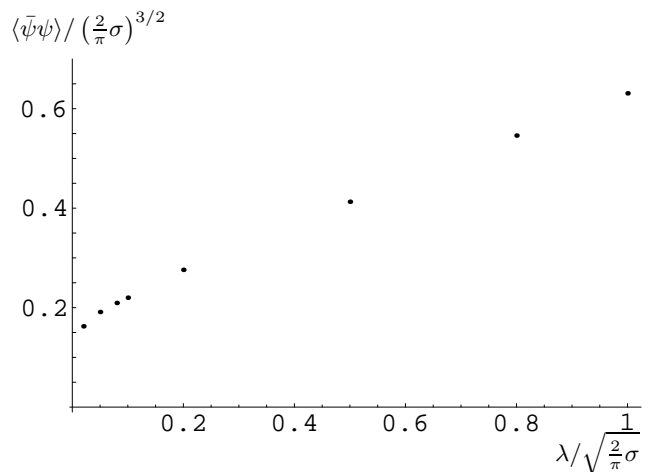


FIG. 4: Testing the convergence of the numerical method with the quark condensate $\langle \bar{\psi}\psi \rangle$.

a single parameter σ . This QM matches the apparently conflicting vector coupling of QCD with a scalar confinement. Our model can be interpreted as a double vertex that couples the quark to the string, or alternatively as a $\gamma_0 S(k) \gamma_0$ vertex. Either way this vertex decomposes in the sum of a scalar vertex 1 and a chiral invariant $\hat{\mathbf{k}} \cdot \boldsymbol{\gamma}$ vertex weighed by simple functions of the dynamical quark mass. In the chiral limit the scalar vertex vanishes, while in the heavy quark limit the confining potential is essentially scalar. Our results for the weighing factors of the scalar vertex and the remaining chiral invariant vertex are shown in Fig. 6.

We solve the mass gap equation for the dynamical generation of the quark mass with the S_{χ} SB, and we in-

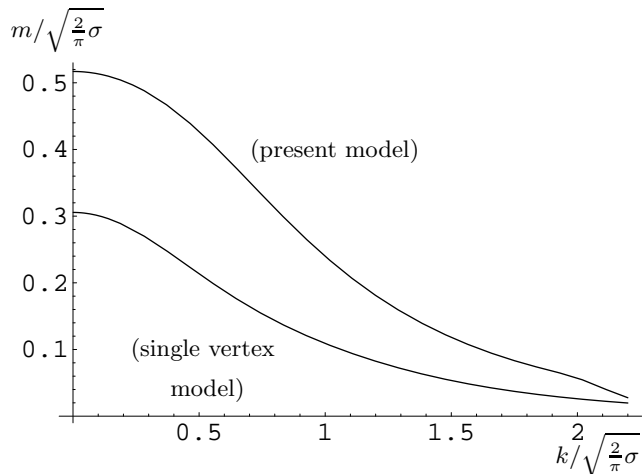


FIG. 5: The m_k solutions of the mass gap equation in units of $\sqrt{\frac{2}{\pi}}\sigma$.

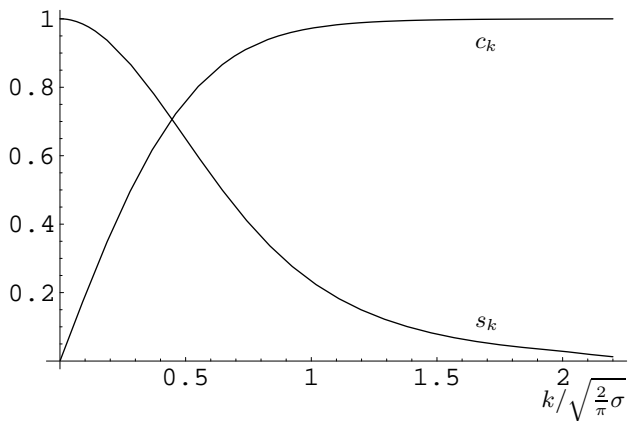


FIG. 6: Form factors for the scalar vertex (s_k) and for the remaining chiral invariant vertex (c_k)

deed generate the constituent quark mass. We show that $S\chi SB$ not only generates a quark mass, but generates also a scalar vertex for the confinement. The results are encouraging because the quark condensate indeed increases when compared with the simpler one vertex vector confining potential.

It is clear that the next step of this work, will consist in adding the shorter range one gluon exchange potential to the confining potential. The resulting model will have two parameters, one for the short range potential, and another one for the confining potential. These parameters will be determined in the fit of the hadron spectrum. In what concerns the mass gap equation, we expect that this will further enhance the quark condensate, possibly up to the expected $-(230 \text{ MeV})^3$.

Acknowledgments

Pedro Bicudo thanks discussions on scalar or string confinement with Alfredo Henriques, Jack Paton, Franz Gross, Dieter Gromes, Nora Brambilla, Jean-François Lagae, Mike Pichowsky, Misha Polikarpov, Dimitri Diakonov and Alexei Nefediev.

The work of G. M. Marques is supported by Fundação para a Ciência e a Tecnologia under the grant SFRH/BD/984/2000.

-
- [1] J. Bjorken, “Why Hadron Physics”, document available at the APS Topical Group on Hadronic Physics, <http://fafnir.phyast.pitt.edu/topical/bj.ps>.
- [2] A. P. Szczepaniak and E. S. Swanson, Phys. Rev. D **55**, 3987 (1997) [arXiv:hep-ph/9611310]; A. P. Szczepaniak and E. S. Swanson, Phys. Rev. D **65**, 025012 (2002) [arXiv:hep-ph/0107078].
- [3] J. F. Lagae, Phys. Lett. B **240**, 451 (1990).
- [4] A. Barchielli, N. Brambilla and G. M. Prosperi, Nuovo Cim. A **103**, 59 (1990).
- [5] N. Brambilla, A. Pineda, J. Soto and A. Vairo, Phys. Rev. D **60**, 091502 (1999) [arXiv:hep-ph/9903355].
- [6] P. Bicudo, Phys. Rev. C **67**, 035201 (2003).
- [7] S. Adler and A. Davis, Nucl. Phys. B **244**, 469 (1984); S. L. Adler, Prog. Theor. Phys. Suppl. **86**, 12 (1986).
- [8] M. S. Bhagwat, M. A. Pichowsky, C. D. Roberts and P. C. Tandy, Phys. Rev. C **68**, 015203 (2003) [arXiv:nucl-th/0304003].
- [9] R. Alkofer and L. von Smekal, Phys. Rept. **353**, 281 (2001) [arXiv:hep-ph/0007355].
- [10] A. B. Henriques, B. H. Kellett and R. G. Moorhouse, Phys. Lett. B **64**, 85 (1976); A. B. Henriques, B. H. Kellett and R. G. Moorhouse, Annals Phys. **93**, 125 (1975); J. Dias de Deus, A. B. Henriques and J. M. Pulido, Z. Phys. C **7**, 157 (1981); A. B. Henriques, Z. Phys. C **11**, 31 (1981).
- [11] L.-H. Chan, Phys. Lett. **71B**, 422 (1977)
- [12] N. Isgur and G. Karl, Phys. Rev. D **18**, 4187 (1978); N. Isgur, Phys. Rev. D **62**, 014025 (2000) [arXiv:hep-ph/9910272].
- [13] W. Kwong, J. L. Rosner and C. Quigg, Ann. Rev. Nucl. Part. Sci. **37**, 325 (1987).
- [14] C. Michael, Phys. Rev. Lett. **56**, 1219 (1986).
- [15] D. Gromes, Z. Phys. C **26**, 401 (1984); W. Lucha, F. F. Schoberl and D. Gromes, Phys. Rept. **200** (1991) 127.
- [16] G. S. Bali, K. Schilling and A. Wachter, Phys. Rev. D **56**, 2566 (1997) [arXiv:hep-lat/9703019].
- [17] T. J. Allen, M. G. Olsson and S. Veseli, Phys. Rev. D **62**, 094021 (2000) [arXiv:hep-ph/0001227].

- [18] N. Isgur and J. Paton, Phys. Rev. D **31**, 2910 (1985); N. Isgur and J. Paton, Phys. Lett. B **124**, 247 (1983).
- [19] F. E. Low, Phys. Rev. D **12**, 163 (1975).
- [20] S. Nussinov, Phys. Rev. Lett. **34**, 1286 (1975).
- [21] Y. A. Simonov, Phys. Atom. Nucl. **60**, 2069 (1997) [Yad. Fiz. **60**, 2252 (1997)] [arXiv:hep-ph/9704301]; Y. A. Simonov, Z. Phys. C **53**, 419 (1992); Y. A. Simonov, Phys. Atom. Nucl. **63**, 94 (2000) [Yad. Fiz. **63**, 106 (2000)]; Y. S. Kalashnikova, A. V. Nefediev and Y. A. Simonov, Phys. Rev. D **64**, 014037 (2001) [arXiv:hep-ph/0103274]; S. M. Fedorov and Y. A. Simonov, arXiv:hep-ph/0306216.
- [22] P. Bicudo, N. Brambilla, E. Ribeiro and A. Vairo, Phys. Lett. B **442**, 349 (1998) [arXiv:hep-ph/9807460].
- [23] A. V. Nefediev, arXiv:hep-ph/0308274.
- [24] F. V. Gubarev, M. I. Polikarpov and V. I. Zakharov, arXiv:hep-th/9812030.
- [25] H. G. Dosch and Y. A. Simonov, Phys. Lett. B **205**, 339 (1988).
- [26] P. J. Bicudo, Phys. Rev. C **60**, 035209 (1999).
- [27] P. J. Bicudo and J. E. Ribeiro, Phys. Rev. D **42**, 1611 (1990).
- [28] P. J. Bicudo, J. E. Ribeiro and A. V. Nefediev, Phys. Rev. D **65**, 085026 (2002) [arXiv:hep-ph/0201173].
- [29] A. Le Yaouanc, L. Oliver, O. Pene and J.-C. Raynal, Phys. Rev. D **29**, 1233 (1984); Phys. Rev. D **31**, 137 (1985). P. J. Bicudo and J. E. Ribeiro, Phys. Rev. D **42**, 1611 (1990).